# Resting and Active Properties of Pyramidal Neurons in Subiculum and CA1 of Rat Hippocampus

NATHAN P. STAFF, HAE-YOON JUNG, TARA THIAGARAJAN, MICHAEL YAO, AND NELSON SPRUSTON
*Department of Neurobiology and Physiology, Institute for Neuroscience, Northwestern University, Evanston, Illinois 60208*

Received 22 March 2000; accepted in final form 8 August 2000

**Staff, Nathan P., Hae-Yoon Jung, Tara Thiagarajan, Michael Yao, and Nelson Spruston.** Resting and active properties of pyramidal neurons in subiculum and CA1 of rat hippocampus. *J Neurophysiol* 84: 2398–2408, 2000. Action potentials are the end product of synaptic integration, a process influenced by resting and active neuronal membrane properties. Diversity in these properties contributes to specialized mechanisms of synaptic integration and action potential firing, which are likely to be of functional significance within neural circuits. In the hippocampus, the majority of subicular pyramidal neurons fire high-frequency bursts of action potentials, whereas CA1 pyramidal neurons exhibit regular spiking behavior when subjected to direct somatic current injection. Using patch-clamp recordings from morphologically identified neurons in hippocampal slices, we analyzed and compared the resting and active membrane properties of pyramidal neurons in the subiculum and CA1 regions of the hippocampus. In response to direct somatic current injection, three subicular firing types were identified (regular spiking, weak bursting, and strong bursting), while all CA1 neurons were regular spiking. Within subiculum strong bursting neurons were found preferentially further away from the CA1 subregion. Input resistance ($R_N$), membrane time constant ($\tau_m$), and depolarizing "sag" in response to hyperpolarizing current pulses were similar in all subicular neurons, while $R_N$ and $\tau_m$ were significantly larger in CA1 neurons. The first spike of all subicular neurons exhibited similar action potential properties; CA1 action potentials exhibited faster rising rates, greater amplitudes, and wider half-widths than subicular action potentials. Therefore both the resting and active properties of CA1 pyramidal neurons are distinct from those of subicular neurons, which form a related class of neurons, differing in their propensity to burst. We also found that both regular spiking subicular and CA1 neurons could be transformed into a burst firing mode by application of a low concentration of 4-aminopyridine, suggesting that in both hippocampal subfields, firing properties are regulated by a slowly inactivating, D-type potassium current. The ability of all subicular pyramidal neurons to burst strengthens the notion that they form a single neuronal class, sharing a burst generating mechanism that is stronger in some cells than others.

## INTRODUCTION

Subiculum, along with presubiculum and parasubiculum, forms an anatomical transition area between the Ammon's Horn region and entorhinal cortex (EC). Subiculum primarily receives axonal input from CA1 and EC layer II/III neurons, and its activity has been shown to be correlated with theta and gamma oscillations as well as with sharp waves of the CA1 region (Chrobak and Buzsaki 1996; Colling et al. 1998). Subiculum has been shown to be the major output center of the hippocampus, to which it belongs, sending parallel projections from various subicular regions to different cortical and subcortical areas (Naber and Witter 1998). Functionally, the principal neurons of the subiculum appear to be "place cells," similar to those of CA1 (Sharp and Green 1994); and in a human magnetic resonance imaging (MRI) study, subiculum was shown to be an area involved in memory retrieval (Gabrieli et al. 1997). Therefore both CA1 and subiculum have been implicated in memory processes and spatial coding, and both are major gateways from the hippocampus to the rest of the brain; however, subiculum has received far less experimental attention.

A major difference between subicular and CA1 pyramidal neurons resides in their firing properties. In response to direct somatic current injection, CA1 pyramidal neurons generate a regular train of action potentials. In the adjacent subiculum, however, most pyramidal neurons have been shown to burst in response to current injection (Behr et al. 1996; Greene and Totterdell 1997; Mason 1993; Mattia et al. 1993; Stewart and Wong 1993; Taube 1993), a phenomenon that has also observed in vivo (Sharp and Green 1994). These different firing properties can have profound implications for the efficacy of information transfer between neurons as well as signaling within a given neuron. For example, given the low probability of synaptic neurotransmitter release, a high-frequency burst entering a presynaptic terminal increases the likelihood of synaptic release per burst to near one (reviewed in Lisman 1997). Similarly, a high-frequency burst backpropagating into the dendrites likely influences synaptic integration and pre-/postsynaptic coincidence detection in ways distinct from a single action potential.

Understanding all the mechanisms by which neurons generate their precise firing properties is a difficult task. The bewildering array of voltage-gated ion channels in the CNS that are activated during action potential generation certainly plays the predominant role in determining a neuron's firing properties. The context in which these ion channels interact, however, is also crucial. Modeling studies have shown that the morphology of a neuron can drastically influence a cell's firing properties. By varying the dendritic arborization while maintaining a steady channel density, a neuron may exhibit either regular spiking or burst firing

Address for reprint requests: N. Spruston, Dept. of Neurobiology and Physiology, Northwestern University, 2153 N. Campus Dr., Evanston, IL 60208-3520 (E-mail: spruston@northwestern.edu).

The costs of publication of this article were defrayed in part by the payment of page charges. The article must therefore be hereby marked "*advertisement*" in accordance with 18 U.S.C. Section 1734 solely to indicate this fact.

 0022-3077/00 $5.00 Copyright © 2000 The American Physiological Society 

(Mainen and Sejnowski 1996). Additionally, subthreshold conductances can contribute significantly to understanding firing properties. For example, in thalamus, the timing of bursts as well as the depolarization leading to the calcium-dependent burst is determined by $I_h$, a current that becomes inactive during action potential generation (reviewed in Steriade et al. 1993).

In addition to their effects on firing properties, dendritic morphology and subthreshold conductances play a key role in the process of synaptic integration. A single pyramidal neuron may receive thousands of excitatory and inhibitory inputs, whose synaptic potentials are sculpted by the neuron's intrinsic morphology and ionic conductances. This transmuted signal is then deciphered near the axon hillock where it becomes the output of the neuron in the form of the action potential. Action potentials backpropagating into the somatodendritic region serve to inform the rest of the neuron about its action potential output, and these are also influenced by cell morphology and ionic conductances. Therefore studying the context in which action potentials occur also provides valuable information about how a neuron integrates its inputs.

To gain an understanding of the intrinsic firing and integrative properties of subicular neurons, we employed patch-clamp techniques and measured resting membrane and firing properties of both subicular and CA1 pyramidal neurons. Although CA1 pyramidal neurons do not burst in response to somatic current injection in vitro, their proximity to subiculum and the abundance of data gathered on these neurons help provide a framework within which burst firing may arise in subiculum.

## METHODS

### *Patch-clamp recording and analysis*

Transverse hippocampal slices (300 $\mu$m) were made from 2- to 9-wk-old Wistar rats. The animals were anesthetized with halothane, and perfused intracardially with ice-cold, oxygenated (bubbled with 95% $O_2$-5% $CO_2$) artificial cerebrospinal fluid (ACSF), containing (in mM) 125 NaCl, 2.5 KCl, 2 $CaCl_2$, 1 $MgCl_2$, 25 $NaHCO_3$, 1.25 $NaH_2PO_4$, and 25 glucose. Throughout the dissection the brains were maintained in ice-cold, oxygenated ACSF. After decapitation, the brains were rapidly removed, and a cut was made on the dorsal surface at a 60° angle to the horizontal plane. The brains were then mounted ventral-side up, and 300-$\mu$m slices (including Ammon's Horn, subiculum and cortex) were prepared using a vibratome (Leica VT 1000S). Slices were incubated for 30 min to 1 h in a holding chamber at 35°C and then stored at room temperature. Individual slices were then transferred to a submerged recording chamber (35 ± 2°C) and visualized with differential interference contrast optics and a Newvicon camera system (Stuart et al. 1993). Somata were selected for recording based on their pyramidal shape and smooth, low-contrast appearance.

Whole cell current-clamp recordings were made from cells using an electrode connected to a bridge amplifier (Dagan BVC-700). Patch-clamp electrodes were pulled from glass capillary tubes, fire polished, and filled with intracellular solution containing (in mM) 115 potassium gluconate, 20 KCl, 10 sodium phosphocreatine, 10 HEPES, 2 EGTA, 2 MgATP, 0.3 NaGTP, and 0.1% biocytin for subsequent determination of morphology. Electrode resistance in the bath ranged from 2 to 7 MΩ, and series resistance ranged from 9 to 35 MΩ. No correction was made for the theoretical junction potential between internal and external solutions. Capacitance compensation and bridge balance were performed. In some experiments, K-$MeSO_4$ was substituted for K-gluconate, and no qualitative difference in burst firing was noted ($n = 3$). Thirty-nine of the 171 subicular neurons were recorded with 10 mM EGTA in the patch solution. The percentage of each of the firing subtypes was equivalent in this group, so all cells were grouped together for use exclusively in the firing property description as well as the anatomical mapping experiments.

In some experiments, perforated-patch recordings were made, for which the pipette solution contained 150 mM KCl, 20 mM tetraethylammonium chloride (TEA), and gramicidin (9 $\mu$g/ml). Perforated-patch recordings were characterized by a gradual reduction in the measured resistance from >1 GΩ (initial seal resistance) to <150 MΩ (input resistance). A precipitous drop in resistance was considered to be indicative of breaking into whole-cell configuration, in which case the recording was discarded. Monitoring spike half-width with inclusion of TEA in the pipette provided an additional means of assessing subtle perforated patch rupture into the whole-cell configuration. In synaptic experiments, stimulation was evoked by current delivered into the alveus through a broken patch pipette filled with ACSF.

Data were transferred during the experiment to a MacIntosh Power PC computer via an ITC 16 digital-analog converter (Instrutech), which was controlled by IGOR Pro Software (Wavemetrics). Subsequent analysis was done off-line using IGOR Pro Software and statistical tests were performed using Excel software (Microsoft). Statistical analysis of multigroup data was performed using a single-factor ANOVA. When there was a significant difference between the groups, Tukey's multicomparison tests were performed to determine the level of significance for each pairwise comparison. All measurements are provided as means ± SE.

### *Biocytin reconstruction and subiculum map*

Neurons filled with biocytin were processed for visualization using an avidin-horseradish peroxidase (HRP) 3,3′-diaminobenzidine reaction. Morphological reconstructions were made using a camera lucida system, whereby each neuron was confirmed to be pyramidal. Morphological analyses were performed on a subset of reconstructed neurons that were examined closely to exclude cells that had obvious dendritic cuttings at the slice surface. Scholl concentric ring analysis was used to provide an estimate of dendritic arborization (Scholl 1953). Twenty-micrometer-diameter concentric rings were superimposed on the camera lucida reconstruction, and numbers of dendritic crossings were counted along both the basal (negative numbers) and apical (positive numbers) dendrites. Measurements of apical dendritic diameter were also performed under ×50 oil magnification at 50-$\mu$m increments from the soma.

The anatomical distribution of subicular neurons within the hippocampal formation was determined for 101 biocytin-filled neurons. Since the neurons were obtained from different slices of different aged rats, a normalized scale corresponding to a subicular map was developed. One axis of the map extended from the CA1-subiculum border to a tangential line connecting the alveus (at the end of subiculum) and dentate gyrus. The other axis extended from the alveus to the hippocampal sulcus (see Fig. 2). Each neuron was then given a normalized *xy* coordinate that corresponded to its relative position within the subiculum. During anatomical measurement, the experimenter was blind to the firing properties of the neuron. Twenty cells processed for morphology were discarded due to unresolvable anatomical borders.

## RESULTS

### *Classification and anatomical distribution of subicular pyramidal neurons*

Whole-cell patch-clamp recordings were obtained from 171 subicular neurons. These neurons were categorized based on

their firing response to a just-suprathreshold, 1-s current injection from the resting potential. Three subtypes were discerned: strong bursting (SB, 88 cells, 51%), weak bursting (WB, 29 cells; 17%) and regular spiking subicular (RS, 54 cells; 32%) neurons (Fig. 1). A burst was defined as two or more action potentials occurring at a high frequency (>200 Hz), followed by an afterhyperpolarization lasting tens of milliseconds. Single bursts were also elicited by short (10 ms) current injections, which resulted in bursts that outlasted the current injections (Fig. 4*B*). SB neurons fired more than one burst (2–7 times) during a 1-s current pulse, whereas WB neurons fired one burst at the beginning of the current pulse and afterward generated a train of single action potentials. RS neurons fired trains of action potentials in response to DC injection. For comparison, recordings were made from 20 CA1 pyramidal neurons, all of which fired regular trains of action potentials in response to DC injection.

Perforated-patch recordings were made to test whether dialysis of the neurons in the whole-cell configuration grossly affected the electrophysiological characteristics of the neurons (see Fig. 7). All three subicular neuronal subtypes were found in the perforated-patch configuration (SB: $n = 7$, WB: $n = 5$, RS: $n = 1$).

To determine whether any differential distribution of the subicular firing types exists within the subiculum, 101 stained subicular neurons (53 SB, 17 WB, 31 RS) were mapped onto a two-dimensional axis system (Fig. 2, see METHODS for description of anatomical measurements). There was a statistically significant effect showing that recordings further away from CA1 (nearer presubiculum) were more likely to be from SB neurons than RS neurons (ANOVA $P < 0.003$). SB and RS neurons were most segregated from each other ($P < 0.005$), while WB neurons overlapped each of the other firing subtypes ($P > 0.2$). Conversely, there was no pattern of distribution of different subicular subtypes with respect to the alveus-hippocampal sulcus axis ($P > 0.7$).

Of the 171 recordings, 121 were processed with a biocytin-avidin-HRP reaction and confirmed to have pyramidal morphology by microscopic examination. Detailed camera lucida drawings were made of six SB, six CA1, five WB, and five RS pyramidal neurons to analyze dendritic morphology. Measurements of apical dendritic diameters were made in 50-$\mu$m increments from the soma, but no differences were found between all pyramidal cell types ($P > 0.7$; grouped data: soma = 15.5 ± 0.4 $\mu$m, 50 $\mu$m = 3.8 ± 0.2 $\mu$m, 100 $\mu$m = 3.65 ± 0.18, 150 $\mu$m = 3.6 ± 0.13 $\mu$m). Scholl analysis, however, revealed a significantly increased amount of dendritic arborization in the proximal apical dendrite of CA1, compared with subicular neurons (Fig. 3, $P < 0.001$).

### *Synaptic responses of strong bursting subicular neurons*

To determine whether bursting can be driven synaptically and to gain an understanding of the synaptic inputs onto subicular neurons, pharmacological dissection of excitatory and inhibitory transmission in SB neurons was employed (Fig. 4). All SB neurons exhibited bursting when stimulated synaptically to threshold ($n = 5$). In some cases, the evoked potential did not reach action potential threshold in control, but application of bicuculline (10 $\mu$M) allowed the synaptic response to reach threshold ($n = 4$) and in some cases increased the number of action potentials within the burst ($n = 3$). The *N*-methyl-D-aspartate (NMDA)-antagonist AP-5 (50 $\mu$M) did not affect bursting ($n = 4$) whereas 6-cyano-7-nitroquinox-

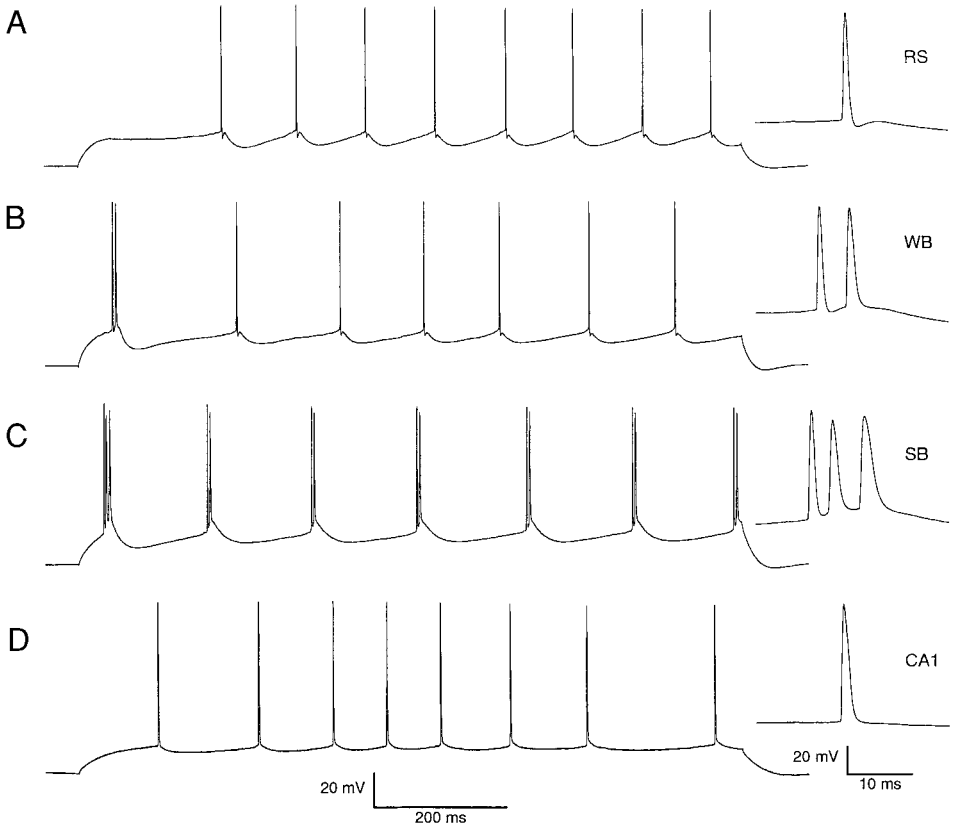


FIG. 1. Generalized responses of CA1 and subicular pyramidal neurons to a 1-s somatic current injection in whole cell patch-clamp configuration. From *top* to *bottom*: regular spiking (RS), weak bursting (WB), strong bursting (SB) subicular and CA1 pyramidal neuron. Injected currents are: RS = 300 pA, SB = 350 pA, RB = 400 pA, CA1 = 200 pA. *Right*: expanded view of 1st action potential or burst.

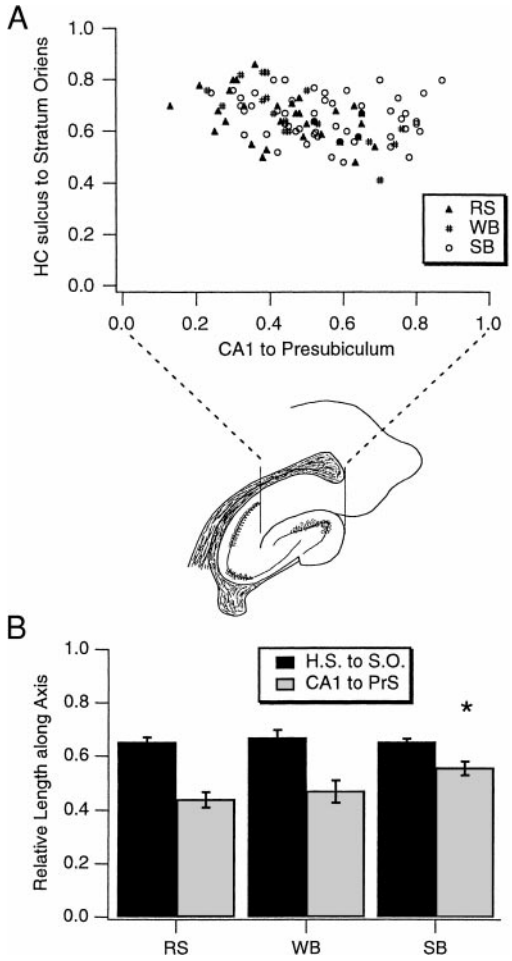


FIG. 2. Anatomical distribution of subicular neuron subtypes. *A*: scatter plot illustrates relative distribution of the different subicular neuron subtypes. In areas further from CA1, an increased tendency to record from SB neurons was noted. Illustration depicts region sampled (see METHODS for details). *B*: bar graph emphasizes that unequal distribution of neurons was noted only in the CA1 to presubiculum (PrS) axis but not along the hippocampal sulcus (H.S.) to stratum oriens (S.O.) axis. Data plotted as means ± SE (* $P < 0.005$, for RS vs. SB).

alene-2,3-dione (CNQX, 2 $\mu$M) mostly abolished excitatory transmission ($n = 2$). These data indicate that SB neurons receive both significant GABA and glutamatergic inputs and that synchronous excitatory stimulation triggers bursting at the threshold for action potential generation.

### *Resting membrane properties of pyramidal neurons*

Resting membrane properties and firing characteristics were analyzed in more detail in a subset of neurons (see Figs. 5 and 6 for illustration and Table 1 for a statistical summary). The resting membrane potential for SB neurons on seal rupture was approximately −67 mV ($n = 15$). Input resistance ($R_N$) was estimated by the slope of a line fitted to the current versus steady-state voltage relationship of current-clamp recordings with low series resistance (<15 MΩ). The average $R_N$ for SB neurons was 37 MΩ ($n = 15$). As illustrated in Fig. 5, during hyperpolarizing current pulses a pronounced depolarizing "sag" occurs (sag ratio = steady-state voltage/peak voltage; the voltage deflection measured is restricted to between 5 and 10 mV). The sag ratio for SB was determined to be 0.79 ($n = 15$). On addition of 5 mM CsCl to the bathing medium this sag is nearly completely abolished, presumably due to a block of the hyperpolarization-activated, nonselective cation conductance ($I_h$). In 5 mM CsCl, the membrane time constant ($\tau_m$) can be more accurately estimated. In SB neurons, $\tau_m = 19$ ms ($n = 5$). The average input resistance in CsCl ($R_{N(Cs^+)}$) accordingly increased to 57 MΩ ($n = 5$).

The resting membrane parameters in WB neurons were nearly identical to those found for SB neurons. The resting membrane potential was about −66 mV ($n = 12$). Input resistance was measured to be 36 MΩ ($n = 12$). WB neurons also had a $Cs^+$-sensitive sag that was the same as in SB neurons (sag ratio = 0.80, $n = 12$). The time constant ($\tau_m$), as measured in 5 mM CsCl was estimated to be 23 ms ($n = 6$), with $R_{N(Cs^+)}$ rising to 75 MΩ.

While RS neurons do not fire bursts of action potentials, their resting membrane properties were the same as those of SB and WB neurons. The resting membrane potential was −67 mV ($n = 13$), $R_N$ was 38 MΩ ($n = 13$), $R_{N(Cs^+)}$ was 75 MΩ ($n = 5$), and $\tau_m$ was 20 ms ($n = 5$). The $Cs^+$-sensitive sag was equivalent as well (sag ratio = 0.79, $n = 13$). When comparing the resting membrane properties ($V_{rest}$, $R_N$, $R_{N(Cs^+)}$, and $\tau_m$) of all three firing subtypes of subicular neurons using a one-factor ANOVA, there were no statistically significant differences among the three firing cell types ($P > 0.35$).

Although CA1 pyramidal neurons have similar morphology, general firing properties, and resting membrane potential (−66 mV, $n = 13$, $P > 0.8$) as RS subicular neurons, their resting membrane properties were strikingly different. The input resistance in control and 5 mM CsCl as well as the membrane time constant in CsCl were all significantly higher in CA1 neurons compared with all subicular firing types [$R_N = 55$ MΩ ($P < 0.001$), $R_{N(Cs^+)} = 120$ MΩ ($P < 0.05$), and $\tau_m = 40$ ms ($P < 0.001$)]. Interestingly, the CA1 sag ratio was identical to the subicular sag (0.79, $n = 15$, $P > 0.9$), implying that the difference in resting conductances between subfields is not due predominantly to a hyperpolarization-activated depolarizing conductance.

### *Action potential properties of pyramidal neurons*

The properties of action potentials in bursting and regular spiking neurons were further analyzed (see Fig. 6 and Table 2 for a statistical summary). Action potential initiation in both subicular and CA1 pyramidal neurons arose from very similar absolute voltages (averages: RS = −47 mV, WB = −45 mV, SB = −47 mV, CA1 = −46 mV, $P > 0.7$), suggesting that there is little difference in the precise mechanism of initial action potential initiation in the different neurons. The current injection required to reach action potential threshold (rheobase) was also similar between subicular and CA1 pyramidal neurons ($P > 0.2$), although there was much variability within and between firing subtypes.

Within a burst, whether coming from a SB or WB neuron, each action potential had stereotyped properties. The number of action potentials within a burst ranged from two to six, and as they progressed the trend was for each action potential to become broader, with slower rates of rise and decay and smaller amplitudes (see Table 2). The first action potential

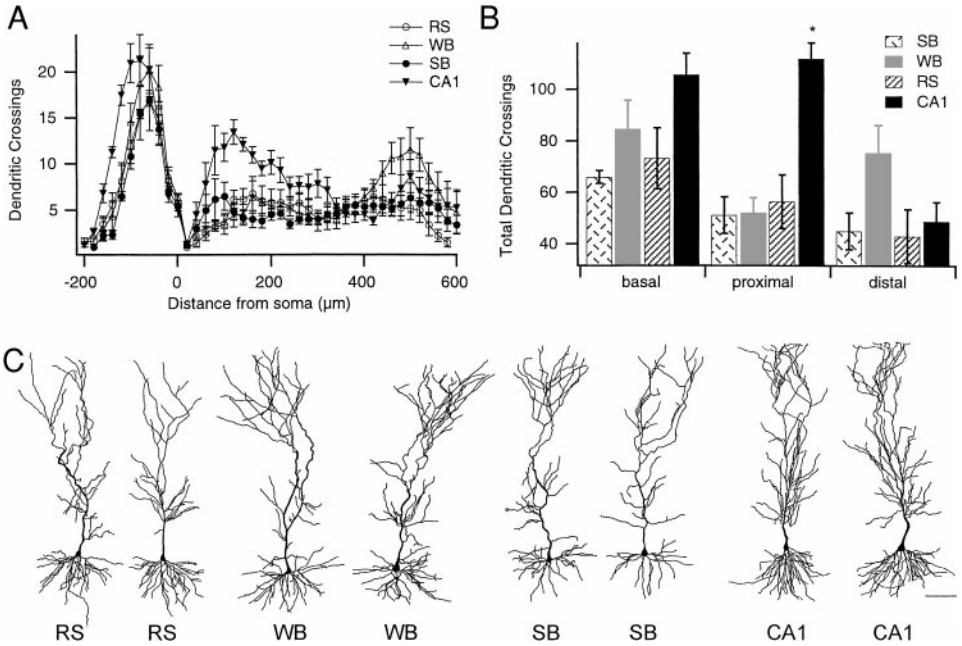


FIG. 3. Morphological analysis of pyramidal neurons. *A*: Scholl analysis plot showing numbers of dendritic crossings along the Scholl rings as a function of distance from soma, SB ($n = 6$), WB ($n = 5$), RS ($n = 5$), CA1 ($n = 6$). *B*: in combined data where crossings were compiled for a given region, CA1 neurons have significantly more dendritic arborization on the proximal apical dendrite than subicular neurons (* $P < 0.001$). Crossings were summed at the basal dendrite level ($-140$ to $-40$ $\mu$m), proximal apical dendrite (60 to 260 $\mu$m), and distal apical dendrite (400 to 540 $\mu$m). *C*: camera lucida drawings of representative pyramidal neurons from the 4 cell types. Scale bar = 100 $\mu$m.

within a burst (either SB or WB) had a half-width of 0.8 ms, which broadened to 1.2 and 1.7 ms in the subsequent spikes. Additionally, as the half-width broadened, so did the interspike interval (Table 2).

Comparing the first action potential of a burst to an action potential in RS neurons again revealed that all subicular neurons had very similar properties yet were distinct from CA1 neurons. The first derivative of $V_m$ ($dV_m/dt$) gives a more sensitive measurement of action potential rising and falling, and the $dV_m/dt$ during the action potential rising phase may correspond to activation of fast voltage-gated $Na^+$ channels (Colbert et al. 1997; Coombs et al. 1957). Using this measure, subicular neurons were found to have similar peak $dV_m/dt$ (rise) (subicular average = 290 mV/ms, $P > 0.4$), while the peak $dV_m/dt$ (rise) of CA1 neurons was significantly faster (CA1 = 380 mV/ms, $P < 0.05$). CA1 neurons also tended to have larger amplitude action potentials than subicular neurons (subiculum average = 93 mV, $P > 0.7$; CA1 = 110 mV, $P < 0.001$). There was no statistically significant difference in the peak rate of action potential descent [peak $dV_m/dt$ (fall)] of all pyramidal neurons measured ($P > 0.2$). The combination of these influences resulted in CA1 neurons displaying a wider half-width than subicular neurons (subiculum average = 0.82 ms, $P > 0.2$; CA1 = 0.95 ms, $P < 0.05$; see Fig. 6, *inset*).

### *Voltage-independence of burst firing*

Other groups have reported that burst firing could be abolished by depolarization of the membrane to near action potential threshold (Mason 1993; Mattia et al. 1997a; Stewart and Wong 1993). We examined this in our study and found that neither depolarization (just below action potential threshold) nor hyperpolarization changed the firing properties of subicular neurons ($n = 30$). This was confirmed in perforated-patch recordings, which obviates concerns about dialysis ($n = 10$, Fig. 7).

### *Regulation of firing mode by potassium currents*

Given that all subicular neurons are alike with regards to all resting and active properties measured, we next tested whether the tendency to burst could be regulated by potassium channels. Bath-application of a low concentration (50 $\mu$M) of 4-AP

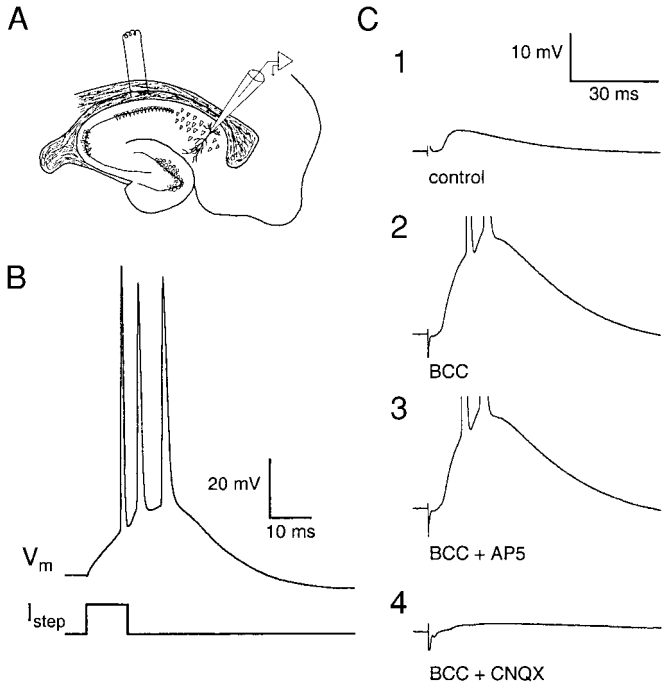


FIG. 4. Synaptic and brief-current responses in a strong bursting neuron. *A*: location of stimulating electrode (alveus) and recording electrode (subiculum). *B*: 10-ms current pulse (500 pA) into SB neuron (different from in *C*), illustrating that the burst outlasts the current injection. *C*: synaptic responses of SB neuron. *C1*: 60-$\mu$A synaptic stimulus in control. *C2*: 60-$\mu$A synaptic stimulus with 10 $\mu$M bicuculline. *C3*: 60-$\mu$A synaptic stimulus with 10 $\mu$M bicuculline and 50 $\mu$M AP-5. *C4*: 100-$\mu$A synaptic stimulus with 10 $\mu$M bicuculline and 2 $\mu$M 6-cyano-7-nitroquinoxalene-2,3-dione (CNQX). Action potentials have been truncated.

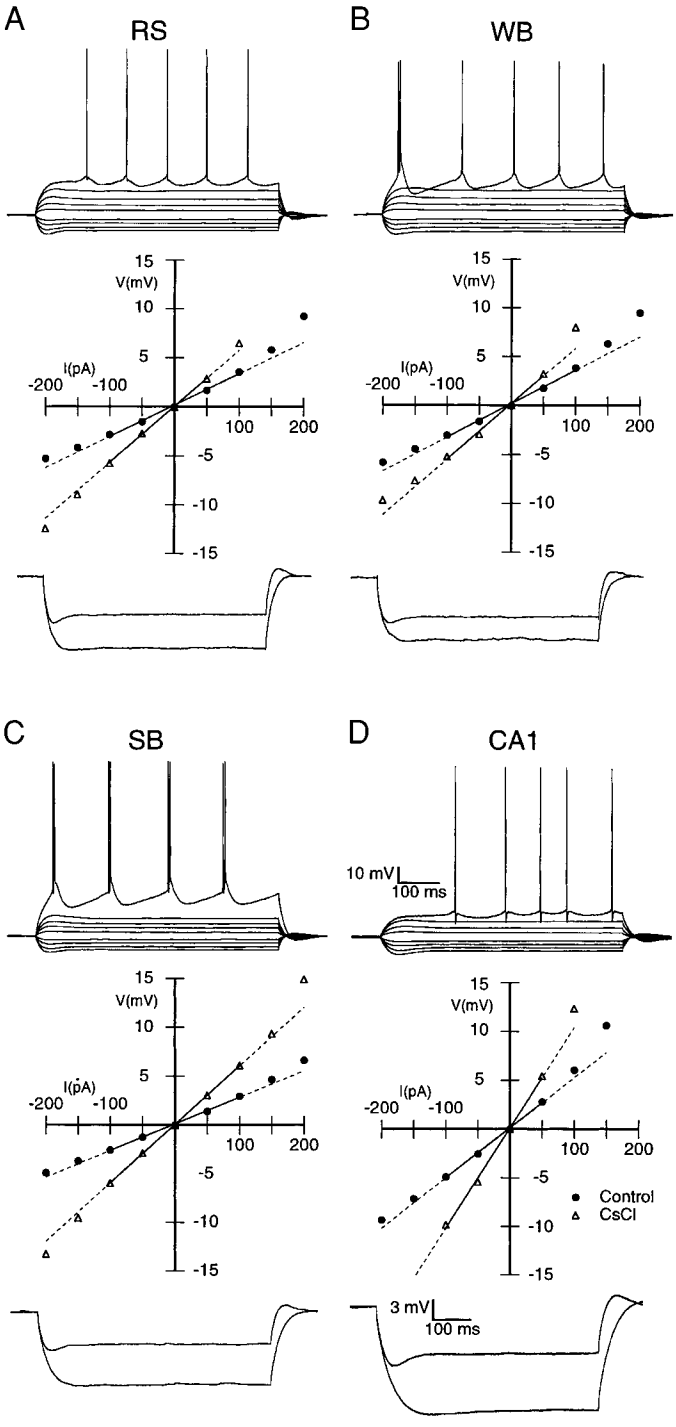


FIG. 5. Current-voltage relationships of pyramidal neurons and the effect of 5 mM CsCl. *Top*: voltage responses to various current steps. *Middle*: *I-V* plot of subthreshold responses in control (●) and in 5 mM CsCl (△). Lines were fit to the linear portion of the *I-V* curve (—) and subsequently extrapolated (- - -). *Bottom*: hyperpolarizing voltage response to a −150-pA, 600-ms current injection in control (*top*) and 5 mM CsCl (*bottom*). *A*: RS subicular neuron (subthreshold = 50-pA steps from −200 to +200 pA; suprathreshold = +250 pA); $R_N$ (control) = 31 MΩ, $R_{N(Cs^+)}$ = 57 MΩ. *B*: WB subicular neuron (subthreshold = 50-pA steps from −200 to +200 pA; suprathreshold = +250 pA); $R_N$ (control) = 34 MΩ, $R_{N(Cs^+)}$ = 57 MΩ. *C*: SB subicular neuron (subthreshold = 50-pA steps from −200 to +200 pA; suprathreshold = +300 pA); $R_N$ (control) = 27 MΩ, $R_{N(Cs^+)}$ = 59 MΩ. *D*: CA1 neuron (subthreshold = 50-pA steps from −200 to +150 pA; suprathreshold = +200 pA); $R_N$ (control) = 51 MΩ, $R_{N(Cs^+)}$ = 102 MΩ.

(a blocker of slowly inactivating, D-type potassium channels) was able to convert four of six RS subicular neurons into strong bursting neurons (Fig. 7); in the other two neurons tested, weak bursting was elicited by 50 μM 4-AP. WB neurons were converted into SB neurons by the same concentration of 4-AP ($n$ = 3). Interestingly, although CA1 neurons are quite distinct from subicular neurons, they too can be converted into bursting neurons by 50 μM 4-AP (5 neurons bursted strongly, 3 bursted weakly, and 1 did not change its firing properties).

## DISCUSSION

This study represents the first patch-clamp analysis of bursting subicular neurons and the first to describe subicular neurons that burst repetitively in response to somatic current injection. Subicular intrinsic bursting is not due to dialysis by whole cell pipette solution since these subtypes were also observed in the less invasive perforated-patch configuration. Although we have classified the neurons into three groups, it may be appropriate to describe the firing properties of subicular neurons as lying along a continuum of propensity to burst. We

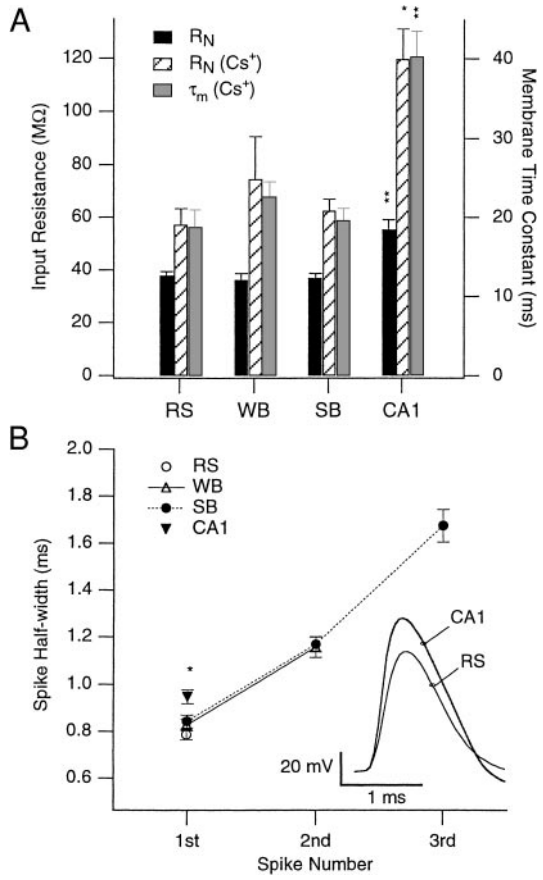


FIG. 6. Passive membrane and firing properties of pyramidal neurons. *A*: input resistances ($R_N$) in control and 5 mM CsCl (*left*) and membrane time constant ($\tau_m$, *right*) for all cell subtypes. While the subicular neurons do not exhibit differences in passive membrane properties, CA1 pyramidal neurons have significantly larger input resistances and accompanying time constants. *B*: half-widths of action potentials from different cell types. The 1st action potential is similar in RS, WB, and SB subicular neuron, with the half-width increasing within a burst. CA1 pyramidal neuron half-width is significantly broader. *Inset*: superimposed action potentials from RS and CA1 neurons illustrating the increased rate of rise, amplitude and half-width. Data plotted as means ± SE, * $P < 0.05$, ** $P < 0.001$.

TABLE 1. *Resting membrane properties*

| | RS | WB | SB | CA1 |
|---|---|---|---|---|
| $V_{rest}$, mV | −66.7 ± 0.8 (13) | −65.6 ± 0.8 (12) | −66.5 ± 0.8 (15) | −66.2 ± 1.1 (13) |
| $R_N$, MΩ | 39.7 ± 1.5 (13) | 36.3 ± 2.5 (12) | 36.9 ± 1.6 (15) | 55.4 ± 3.7 (13) |
| sag ratio | 0.79 ± 0.02 (13) | 0.80 ± 0.02 (12) | 0.79 ± 0.01 (15) | 0.79 ± 0.01 (15) |
| $R_{N(Cs^+)}$, MΩ | 62.6 ± 6.3 (5) | 74.6 ± 16.1 (5) | 57.2 ± 4.5 (5) | 119.8 ± 11.6 (8) |
| $\tau_{m(Cs^+)}$, ms | 19.6 ± 2.2 (5) | 22.6 ± 2.0 (6) | 18.8 ± 1.6 (5) | 40.3 ± 3.2 (8) |

Values are means ± SE; *n* is in parentheses.

observed a wide assortment of firing properties, ranging from neurons that never burst to those that would burst repetitively (7 times in 1 s, with >3 spikes per burst), with nearly all varieties in between (an example being a neuron that burst twice and then spiked regularly, which was classified as SB). Despite the variety in firing modalities, however, subicular neurons belong to a homogenous group with respect to all other measured parameters (both resting and active, see Tables 1 and 2).

An interesting observation of this study is that neurons further away from CA1 are more likely to burst, although we did not reproduce a previous study that found more RS subicular neurons nearer the hippocampal sulcus (Greene and Totterdell 1997). Different subfields of subiculum (proximal to CA1 vs. distal to CA1) have been shown to preferentially receive input from different CA1 regions (reviewed in Amaral 1993). Specifically, proximal CA1 (with respect to CA3) innervates distal subiculum, whereas distal CA1 innervates proximal subiculum. Likewise efferent projections from restricted portions of subiculum (which can be further segregated into dorsal vs. ventral subiculum as well as proximal vs. distal) send parallel inputs to a wide array of cortical and subcortical structures (Naber and Witter 1998). It may be that the firing properties of subicular neurons serve to segregate subicular output one level further. In fact, there is some evidence that regular spiking and bursting subicular neurons may project differentially to entorhinal cortex and presubiculum, respectively (Stewart 1997).

### *Comparison of subicular and CA1 pyramidal neurons*

MORPHOLOGY. Analysis of the dendritic morphologies of pyramidal neurons in subiculum and CA1 revealed that CA1 neurons have significantly more oblique branches arising from the proximal apical dendrite than subicular neurons. It could be that this difference contributes to the firing properties of the two hippocampal regions. In published models, however, increased dendritic membrane surface area augments the propensity to burst (Mainen and Sejnowski 1996). It may also be that the different levels of proximal apical oblique branches are related to differences in synaptic input into the subicular and CA1 regions.

RESTING PROPERTIES. In this study 68% of the 171 subicular neurons exhibited intrinsic bursting behavior. By contrast, none of the 20 CA1 neurons we recorded from exhibited bursting behavior. With respect to resting properties, all subicular neurons have nearly identical $R_N$, $R_{N(Cs^+)}$, and $\tau_m$, all of which are significantly different from those measured in CA1 pyramidal neurons.

Overall, subicular pyramidal neurons have greater resting conductances than CA1 pyramidal neurons as measured by $R_N$, $R_{N(Cs^+)}$, and $\tau_m$. These conductances can be divided into $Cs^+$-sensitive and -insensitive portions. In the presence of 5 mM CsCl, subicular neurons still have a much smaller input resistance than in CA1, demonstrating that there is a greater amount of resting $Cs^+$-insensitive conductances in subiculum.

TABLE 2. *Action potential properties*

| | RS | WB | SB | CA1 |
|---|---|---|---|---|
| Spike threshold, mV | −46.6 ± 0.9 (12) | −45.2 ± 0.6 (12) | −46.8 ± 0.8 (20) | −46.3 ± 0.6 (20) |
| Rheobase, pA | 283 ± 28 (12) | 314 ± 34 (12) | 234 ± 14 (20) | 213 ± 21 (20) |
| Half-width, ms | | | | |
| 1st spike | 0.79 ± 0.02 (26) | 0.83 ± 0.03 (15) | 0.84 ± 0.03 (36) | 0.95 ± 0.03 (20) |
| 2nd spike | — | 1.16 ± 0.04 (15) | 1.17 ± 0.03 (36) | — |
| 3rd spike | — | 0.84 ± 0.03 (13)* | 1.68 ± 0.07 (14) | — |
| Amplitude, mV | | | | |
| 1st spike | 95.4 ± 2.3 (12) | 90.2 ± 2.9 (12) | 93.0 ± 3.3 (20) | 112.0 ± 9.0 (20) |
| 2nd spike | — | 87.6 ± 2.4 (12) | 87.2 ± 2.5 (20) | — |
| 3rd spike | — | 90.5 ± 2.9 (12)* | 79.7 ± 4.0 (8) | — |
| Peak $dV_m/dt$, rise | | | | |
| 1st spike | 299 ± 17 (12) | 264 ± 18 (12) | 297 ± 22 (20) | 381 ± 18 (20) |
| 2nd spike | — | 208 ± 15 (12) | 217 ± 15 (20) | — |
| 3rd spike | — | 254 ± 17 (12)* | 176 ± 18 (8) | — |
| Peak $dV_m/dt$, fall | | | | |
| 1st spike | −110 ± 5.0 (12) | −88.8 ± 5.1 (12) | −103 ± 5 (20) | −94.8 ± 4.7 (20) |
| 2nd spike | — | −51.6 ± 3.3 (12) | −53.3 ± 2.0 (20) | — |
| 3rd spike | — | −87.3 ± 5.4 (12)* | −38.2 ± 3.1 (8) | — |
| Interspike interval, ms | | | | |
| 1st | — | 4.73 ± 0.17 (15) | 4.09 ± 0.12 (35) | — |
| 2nd | — | — | 5.40 ± 0.41 (14) | — |

Values are means ± SE; *n* is in parentheses. * Single action potential following a burst.

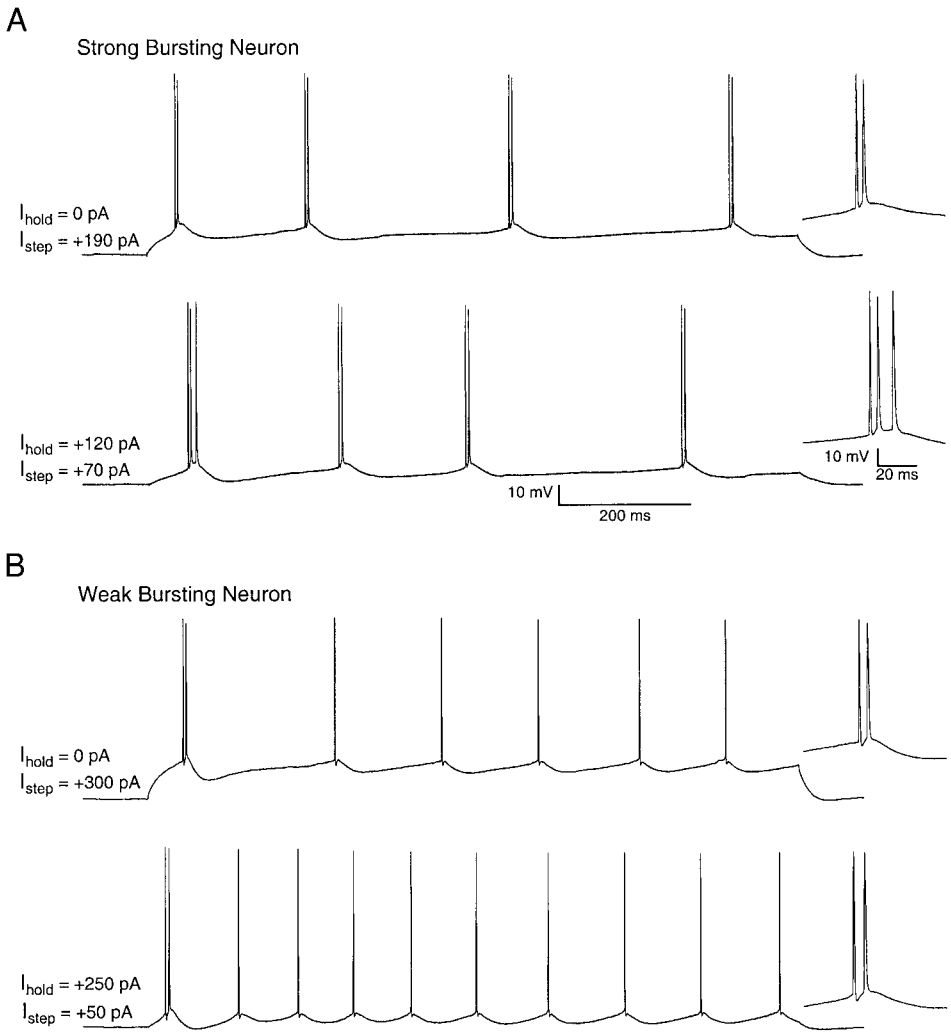


FIG. 7. Voltage-independence of bursting in perforated-patch recordings. *A*, *top*: SB neuron without any holding current exhibits bursting with 190-pA current injection. *Bottom*: when depolarized to just under threshold by 120-pA holding current, bursting persists. *B*, *top*: WB neuron without any holding current exhibits bursting with 300-pA current injection. *Bottom*: when depolarized to just under threshold by 250-pA holding current, bursting also persists.

Levels of the $Cs^+$-sensitive conductance, on the other hand, appear to be equivalent between all cell types. A majority of the $Cs^+$-sensitive conductance is carried by the hyperpolarization-activated, nonselective cation current, $I_h$, which is active at resting membrane potentials and does not inactivate (Magee 1998).

In CA1, subthreshold synaptic integration has been studied extensively, and $I_h$ has been shown to be important in regulating temporal summation. There is an increasing density of $I_h$ distally along the apical dendrite, and it has been shown that during excitatory postsynaptic potentials, the deactivation of $I_h$ delivers a net hyperpolarization helping to prevent temporal summation at frequencies $<$100 Hz (Magee 1998, 1999). It will be interesting to determine whether $I_h$ performs a similar function in subiculum, where its increased resting, non-$I_h$-derived conductances also shape synaptic integration. Given that subicular neurons have a faster $\tau_m$, the hyperpolarizing effects of $I_h$ deactivation may not be as important since the membrane will already repolarize quicker than in CA1 neurons. Recording the currents along the somatodendritic axis, as well as performing dual recordings to examine synaptic integration, will certainly shed light on these issues.

ACTIVE PROPERTIES. During action potential generation, the fastest rising phase of the spike likely corresponds to a time of maximal $Na^+$ channel activation, prior to significant $Na^+$ channel inactivation and subsequent activation of repolarizing $K^+$ channels. By using the first derivative of the action potential rise [$dV_m/dt$ (rise)], one can more directly measure the fastest portion of the action potential and compare it between cell types. We observed that the first action potential of a subicular neuron (whether in a train or a burst) has a similar peak $dV_m/dt$ (rise) across firing types, suggesting that the density of fast voltage-gated $Na^+$ channels does not account for differences in the tendency of subicular neurons to burst. This does not, however, rule out an influence of a persistent $Na^+$ current on bursting, which would not likely affect measurement of $dV_m/dt$ (rise). As a caveat, it should be noted the action potentials recorded at the soma are likely backpropagated from the axon (Colbert and Johnston 1996; Spruston et al. 1995). Therefore the action potentials recorded in the soma have already been shaped by geometry and intrinsic conductances of the soma and do not necessarily reflect what action potentials look like in the axon (Williams and Stuart 1999). However, given that both the absolute voltage threshold for action potentials as well as the resting parameters were similar across all subicular neurons, it is likely that $dV_m/dt$ (rise) can be used for comparisons.

The action potentials recorded in the somata of subicular

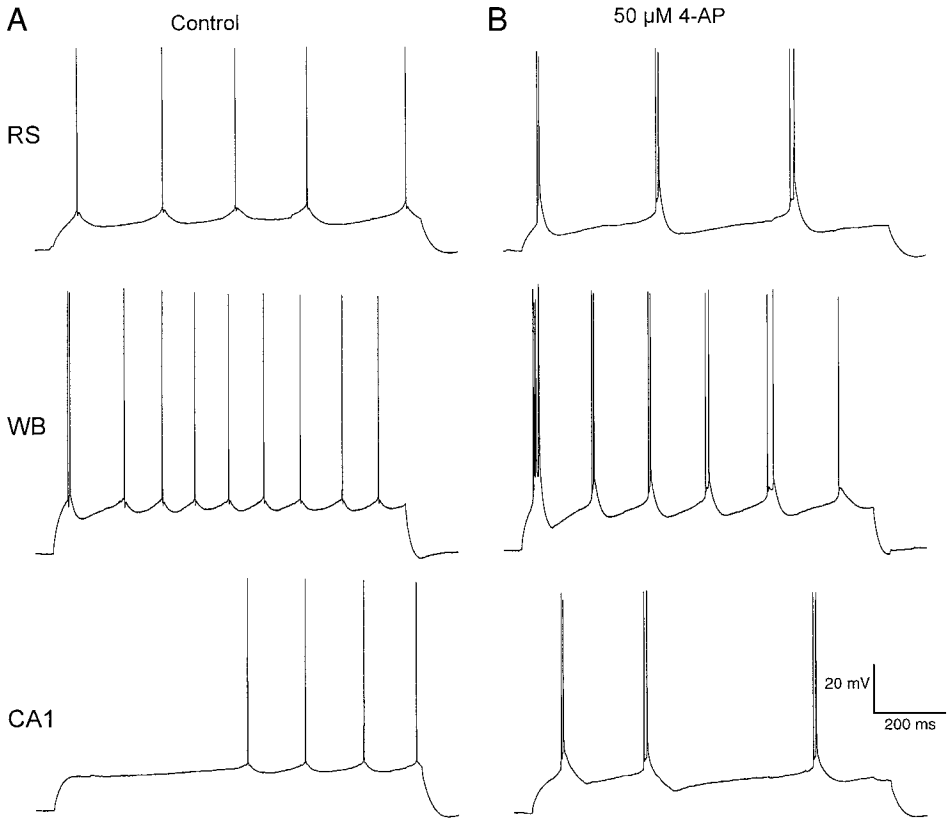


FIG. 8. Potassium conductances regulate firing mode of CA1 and subicular neurons. *A*: control traces from RS (90 pA), WB (330 pA), and CA1 (280 pA) pyramidal neurons. *B*: recordings in the same neurons in the presence of 50 $\mu$M 4-aminopyridine (4-AP; RS = 100 pA, WB = 290 pA, CA1 = 220 pA).

and CA1 pyramidal neurons were observed to be quite different, with subicular action potentials having slower rising rates, smaller amplitudes, and smaller half-widths than observed in CA1 neurons. Given that subicular axonal action potentials have greater attenuation measured at the soma than CA1 neurons, perhaps action potentials correspondingly do not backpropagate into distal dendrites as effectively in subiculum compared with CA1 (or perhaps the action potentials are different from the start in the axon, although they do arise from the same voltage threshold).

### *Bursting in subiculum*

Using patch-clamp recording, we have observed three electrophysiological subtypes of subicular neurons based on their action potential firing in response to a just suprathreshold, 1-s somatic current pulse. These subicular subtypes are regular spiking (RS), weak bursting (WB; an initial burst followed by regular spiking action potentials), and strong bursting (SB; repetitively bursting). Others have recorded from subicular neurons with sharp microelectrodes but only observed WB and RS firing subtypes (Greene and Totterdell 1997; Mason 1993; Mattia et al. 1993; Stewart and Wong 1993; Taube 1993). All but one of those studies found similar resting membrane properties between bursting and nonbursting neurons. Our measurements of $R_N$, $R_{N(Cs^+)}$, and $\tau_m$ are larger than those found in earlier studies, which is likely due to the somatic shunt introduced by sharp microelectrode impalement (Spruston and Johnston 1992; Staley et al. 1992). Stewart and Wong (1993) described a type of regular spiking neuron that had markedly different properties (little sag and longer $\tau_m$) than those described here and elsewhere. We did not find any neurons that fit the characteristics they described.

Our recordings show that subicular bursting is not affected by depolarization or hyperpolarization of the membrane potential, a finding observed both in whole-cell and perforated-patch configurations. This is in conflict with previous studies using sharp microelectrodes, which found that depolarization prevented burst formation in subicular neurons (Mason 1993; Mattia et al. 1997; Stewart and Wong 1993). It is hard to reconcile this difference, though we note that these studies did not observe SB neurons, so perhaps bursting was not as robust in their preparation and therefore easier to prevent.

Our recordings suggest that all subicular pyramidal neurons are able to burst. Two-thirds of subicular neurons burst intrinsically to a varying degree, while the remainder burst when exposed to the D-type potassium current blocker 50 $\mu$M 4-AP. Based on the remarkable similarity between groups, it seems unlikely that resting membrane properties contribute significantly to the differences in firing subtypes in subiculum. Additionally, we did not find any obvious morphological differences in the dendritic arborization that could readily account for different firing properties (Mainen and Sejnowski 1996).

The ionic mechanisms of bursting in subiculum have been debated in the literature. In a series of papers, Mattia and collaborators have proposed that a $Na^+$ current is responsible for the slow depolarizing envelope that underlies a burst (Mattia et al. 1993, 1997a,b). On the other hand, Stewart and Wong suggested a $Ca^{2+}$ current is necessary for the burst (Stewart and Wong 1993). To resolve this controversy, these implicated currents will need to be measured directly with voltage-clamp procedures (Jung et al. 1999).

### *Bursting in CA1*

CA1 pyramidal neurons have been studied extensively in the whole-cell patch-clamp configuration in vitro, and they do not burst in response to just-suprathreshold somatic currents injection in normal ACSF (Golding et al. 1999). However, other groups have reported intrinsic bursting at threshold in the CA1 region using sharp microelectrodes (Jensen et al. 1994; Kandel and Spencer 1961; Masukawa et al. 1982; Schwartzkroin 1975). Using pharmacological dissection of $Na^+$ and $Ca^{2+}$ currents, Yaari and collaborators have suggested that this intrinsic "threshold bursting" is dependent on a persistent $Na^+$ current (Azouz et al. 1996). Furthermore this threshold bursting can be enhanced when external potassium is raised from 3.5 to 7.5 mM (Jensen et al. 1994). It is unclear what accounts for the discrepancy in intrinsic firing properties when comparing sharp microelectrode versus patch-clamp recording techniques, although perforated-patch recordings from CA1 neurons also do not show threshold bursting (Spruston and Johnston 1992).

It has been demonstrated that, in vivo, CA1 pyramidal neurons exhibit complex spike bursting, a type of bursting which has been correlated with sharp waves in field recordings. These complex spike bursts are quite different from threshold bursting. Complex spike bursts require either strong synchronous synaptic inputs to the dendrites or strong direct dendritic current injection (Golding et al. 1999). Threshold bursting in subicular neurons, by contrast, requires only a suprathreshold somatic current injection. Complex spike bursts have been shown both in vivo and in vitro to be derived from dendritic electrogenesis, in the form of large regenerative $Ca^{2+}$ and $Na^+$ spikes (Golding and Spruston 1998; Golding et al. 1999; Kamondi et al. 1998). Recordings at the soma during these complex spikes often show a burst of action potentials.

In a recent study, Golding et al. demonstrated that bath-applied 100 $\mu$M 4-AP permitted a just-suprathreshold somatic current injection to produce a burst of action potentials (in contrast with the synchronized dendritic depolarization normally necessary for CA1 complex spike bursting). In normal ACSF, bursts are not produced by somatic current injection; rather, somatic current injection stimulates backpropagating action potentials, which activate dendritic A-type (early in a train) and D-type potassium currents (later in a train) (Golding et al. 1999; Hoffman et al. 1997; Magee and Carruth 1999). These currents provide a shunt that prevents dendritic $Ca^{2+}$ spikes, such as those described for complex spikes. When a low concentration of 4-AP is present, however, backpropagating action potentials provide sufficient dendritic depolarization to elicit a dendritic $Ca^{2+}$ spike, which, in turn, produces a somatic burst of action potentials. In the present study, low concentrations of a D-type potassium current blocker (50 $\mu$M 4-AP) usually converted a regular spiking CA1 pyramidal neuron into a threshold bursting neuron. It may be that the CA1 threshold bursting reported in our study involves a similar dendritic $Ca^{2+}$ electrogenesis, although we cannot rule out that there may be some contribution of a persistent-$Na^+$ current (Azouz et al. 1996). Furthermore it remains to be seen whether dendritic calcium electrogenesis underlies the mechanism for bursting in subiculum, as it does in bursting layer 5 cortical pyramidal neurons (Larkum et al. 1999; Schwindt and Crill 1999; Williams and Stuart 1999, but see Guatteo et al. 1996).

### *Functional implications of subicular intrinsic bursting*

There has been much speculation about the functional relevance of action potential bursting. Primarily, it has been suggested that bursting increases the probability of synaptic vesicle release at the presynaptic terminal (reviewed in Lisman 1997). This has been demonstrated directly in paired recordings from neocortical neurons, where it was shown that each action potential within a burst is transmitted to the presynaptic terminal and may result in synaptic release (Williams and Stuart 1999). Using minimal stimulation techniques in the Schaffer collateral to CA1 pyramidal synapse, it has been shown that high-frequency stimulation mimicking a burst ensures neurotransmitter release (Dobrunz et al. 1997).

It has also been hypothesized that bursting provides specific information content that is not found in general action potential activity. For instance, in "place cells" of the CA1 region, action potential bursting defines a more restricted place field within that described merely by the cells firing rate (Otto et al. 1991). CA1 bursting has also been correlated to consummatory behavior and slow-wave sleep, where the function of bursting versus tonic firing is less clear (Buzsaki 1986). Another example of the information content of bursting is the thalamus, where bursting is a network-driven phenomenon that is seen predominantly during sleep, but it also may be involved in the trance-like condition of absence seizures (Steriade et al. 1993).

The significance of bursting in subiculum, a phenomenon observed both in vitro and in vivo, is still largely unexplored. Subiculum is involved in both spatial and declarative memory processing (Gabrieli et al. 1997; Sharp 1999). It has been described as a relay center for the processed information of the hippocampus and also as a possible location of epileptogenesis. Given its role as a major output of the hippocampus, in combination with its dual entorhinal and CA1 input, one idea is that subiculum may serve to gate information flow out of the hippocampus, akin to thalamic gating of cortical flow. Subicular bursting and the resultant unerring synaptic release would ensure that the processed information reliably passes onto the next level of circuitry. Understanding the basic mechanisms of how these neurons generate their bursts and how bursting can be manipulated will certainly be a key to understanding subiculum's place within the hippocampal formation and will provide valuable information about hippocampal processing as a whole.

We thank D. Cooper, N. Golding, and T. Mickus for critical reading of the manuscript.

This work was supported by grants from the National Institute of Neurological Disorders and Stroke (NS-35180), the National Science Foundation (IBN-9876032), the Human Frontiers in Science Program, and the Sloan and Klingenstein Foundations (N. Spruston).

## REFERENCES

AMARAL DG. Emerging principles of intrinsic hippocampal organization. *Curr Opin Neurobiol* 3: 225–229, 1993.

AZOUZ R, JENSEN MS, AND YAARI Y. Ionic basis of spike after-depolarization and burst generation in adult rat hippocampal CA1 pyramidal cells. *J Physiol (Lond)* 492: 211–223, 1996.

BEHR J, EMPSON RM, SCHMITZ D, GLOVELI T, AND HEINEMANN U. Electrophysiological properties of rat subicular neurons in vitro. *Neurosci Lett* 220: 41–44, 1996.

BUZSAKI G. Hippocampal sharp waves: their origin and significance. *Brain Res* 398: 242–252, 1986.

CHROBAK JJ AND BUZSAKI G. High-frequency oscillations in the output networks of the hippocampal-entorhinal axis of the freely behaving rat. *J Neurosci* 16: 3056–3066, 1996.

COLBERT CM AND JOHNSTON D. Axonal action-potential initiation and $Na^+$ channel densities in the soma and axon initial segment of subicular pyramidal neurons. *J Neurosci* 16: 6676–6686, 1996.

COLBERT CM, MAGEE JC, HOFFMAN DA, AND JOHNSTON D. Slow recovery from inactivation of $Na^+$ channels underlies the activity-dependent attenuation of dendritic action potentials in hippocampal CA1 pyramidal neurons. *J Neurosci* 17: 6512–6521, 1997.

COLLING SB, STANFORD IM, TRAUB RD, AND JEFFERYS JG. Limbic gamma rhythms. I. Phase-locked oscillations in hippocampal CA1 and subiculum. *J Neurophysiol* 80: 155–161, 1998.

COOMBS JS, CURTIS DR, AND ECCLES JC. The generation of impulses in motoneurones. *J Physiol (Lond)* 139: 232–249, 1957.

DOBRUNZ LE, HUANG EP, AND STEVENS CF. Very short-term plasticity in hippocampal synapses. *Proc Natl Acad Sci USA* 94: 14843–14847, 1997.

GABRIELI JDE, BREWER JB, DESMOND JE, AND GLOVER GH. Separate neural bases of two fundamental memory processes in the human medial temporal lobe. *Science* 276: 264–266, 1997.

GOLDING NL, JUNG H, MICKUS T, AND SPRUSTON N. Dendritic calcium spike initiation and repolarization are controlled by distinct potassium channel subtypes in CA1 pyramidal neurons. *J Neurosci* 19: 8789–8798, 1999.

GOLDING NL AND SPRUSTON N. Dendritic sodium spikes are variable triggers of axonal action potentials in hippocampal CA1 pyramidal neurons. *Neuron* 21: 1189–1200, 1998.

GREENE JR AND TOTTERDELL S. Morphology and distribution of electrophysiologically defined classes of pyramidal and nonpyramidal neurons in rat ventral subiculum in vitro. *J Comp Neurol* 380: 395–408, 1997.

GUATTEO E, FRANCESCHETTI S, BACCI A, AVANZINI G, AND WANKE E. A TTX-sensitive conductance underlying burst firing in isolated pyramidal neurons from rat neocortex. *Brain Res* 741: 1–12, 1996.

HOFFMAN DA, MAGEE JC, COLBERT CM, AND JOHNSTON D. $K^+$ channel regulation of signal propagation in dendrites of hippocampal pyramidal neurons. *Nature* 387: 869–875, 1997.

JENSEN MS, AZOUZ R, AND YAARI Y. Variant firing patterns in rat hippocampal pyramidal cells modulated by extracellular potassium. *J Neurophysiol* 71: 831–839, 1994.

JUNG H, MICKUS T, AND SPRUSTON N. Prolonged sodium channel inactivation contributes to dendritic action potential attenuation in hippocampal pyramidal neurons. *J Neurosci* 17: 6639–6646, 1997.

JUNG H, STAFF N, AND SPRUSTON N. Ionic basis of intrinsic bursting in rat subicular neurons. *Soc Neurosci Abstr* 25: 1740, 1999.

KAMONDI A, ACSADY L, AND BUZSAKI G. Dendritic spikes are enhanced by cooperative network activity in the intact hippocampus. *J Neurosci* 18: 3919–3928, 1998.

KANDEL ER AND SPENCER WA. Electrophysiology of hippocampal neurons. II. after potentials and repetitive firing. *J Neurophysiol* 24: 243–259, 1961.

LARKUM ME, ZHU JJ, AND SAKMANN B. A new cellular mechanism for coupling inputs arriving at different cortical layers. *Nature* 398: 338–341, 1999.

LISMAN JE. Bursts as a unit of neural information: making unreliable synapses reliable. *Trends Neurosci* 20: 38–43, 1997.

MAGEE JC. Dendritic hyperpolarization-activated currents modify the integrative properties of hippocampal CA1 pyramidal neurons. *J Neurosci* 18: 7613–7624, 1998.

MAGEE JC. Dendritic $I_h$ normalizes temporal summation in hippocampal CA1 neurons. *Nat Neurosci* 2: 508–514, 1999.

MAGEE JC AND CARRUTH M. Dendritic voltage-gated ion channels regulate the action potential firing mode of hippocampal CA1 pyramidal neurons. *J Neurophysiol* 82: 1895–1901, 1999.

MAGEE JC AND JOHNSTON D. A synaptically controlled, associative signal for Hebbian plasticity in hippocampal neurons. *Science* 275: 209–213, 1997.

MAINEN ZF AND SEJNOWSKI TJ. Influence of dendritic structure on firing pattern in model neocortical neurons. *Nature* 382: 363–366, 1996.

MASON A. Electrophysiology and burst-firing of rat subicular pyramidal neurons in vitro: a comparison with area CA1. *Brain Res* 600: 174–178, 1993.

MASUKAWA LM, BENARDO LS, AND PRINCE DA. Variations in electrophysiological properties of hippocampal neurons in different subfields. *Brain Res* 242: 341–344, 1982.

MATTIA D, HWA GG, AND AVOLI M. Membrane properties of rat subicular neurons in vitro. *J Neurophysiol* 70: 1244–1248, 1993.

MATTIA D, KAWASAKI H, AND AVOLI M. In vitro electrophysiology of rat subicular bursting neurons. *Hippocampus* 7: 48–57, 1997a.

MATTIA D, KAWASAKI H, AND AVOLI M. Repetitive firing and oscillatory activity of pyramidal-like bursting neurons in the rat subiculum. *Exp Brain Res* 114: 507–517, 1997b.

MICKUS T, JUNG H, AND SPRUSTON N. Properties of slow, cumulative sodium channel inactivation in rat hippocampal CA1 pyramidal neurons. *Biophys J* 76: 846–860, 1999.

NABER PA AND WITTER MP. Subicular efferents are organized mostly as parallel projections: a double-labeling, retrograde-tracing study in the rat. *J Comp Neurol* 393: 284–297, 1998.

OTTO T, EICHENBAUM H, WIENER SI, AND WIBLE CG. Learning-related patterns of CA1 spike trains parallel stimulation parameters optimal for inducing hippocampal long-term potentiation. *Hippocampus* 1: 181–192, 1991.

SCHOLL D. Dendritic organization in the neurons of the visual and motor cortices of the rat. *J Anat* 87: 387–406, 1953.

SCHWARTZKROIN PA. Characteristics of CA1 neurons recorded intracellularly in the hippocampal in vitro slice preparation. *Brain Res* 85: 423–436, 1975.

SCHWINDT P AND CRILL W. Mechanisms underlying burst and regular spiking evoked by dendritic depolarization in layer 5 cortical pyramidal neurons. *J Neurophysiol* 81: 1341–1354, 1999.

SHARP PE. Comparison of the timing of hippocampal and subicular spatial signals: implications for path integration. *Hippocampus* 9: 158–172, 1999.

SHARP PE AND GREEN C. Spatial correlates of firing patterns of single cells in the subiculum of the freely moving rat. *J Neurosci* 14: 2339–2356, 1994.

SPRUSTON N AND JOHNSTON D. Perforated patch-clamp analysis of the passive membrane properties of three classes of hippocampal neurons. *J Neurophysiol* 67: 508–529, 1992.

SPRUSTON N, SCHILLER Y, STUART G, AND SAKMANN B. Activity-dependent action potential invasion and calcium influx into hippocampal CA1 dendrites. *Science* 268: 297–300, 1995.

STALEY KJ, OTIS TS, AND MODY I. Membrane properties of dentate gyrus granule cells: comparison of sharp microelectrode and whole-cell recordings. *J Neurophysiol* 67: 1346–1358, 1992.

STERIADE M, MCCORMICK DA, AND SEJNOWSKI TJ. Thalamocortical oscillations in the sleeping and aroused brain. *Science* 262: 679–685, 1993.

STEWART M. Antidromic and orthodromic responses by subicular neurons in rat brain slices. *Brain Res* 769: 71–85, 1997.

STEWART M AND WONG RK. Intrinsic properties and evoked responses of guinea pig subicular neurons in vitro. *J Neurophysiol* 70: 232–245, 1993.

STUART GJ, DODT HU, AND SAKMANN B. Patch-clamp recordings from the soma and dendrites of neurons in brain slices using infrared video microscopy. *Pflügers Arch* 423: 511–518, 1993.

TAUBE JS. Electrophysiological properties of neurons in the rat subiculum in vitro. *Exp Brain Res* 96: 304–318, 1993.

WILLIAMS SR AND STUART GJ. Mechanisms and consequences of action potential burst firing in rat neocortical pyramidal neurons. *J Physiol (Lond)* 52: 467–482, 1999.